Journal of Applied Sciences

ISSN 1812-5654

science alert

ANSInet
an open access publisher
http://ansinet.com

Journal of Applied Sciences 14 (22): 3083-3088, 2014
ISSN 1812-5654 / DOI: 10.3923/jas.2014.3083.3088

Effects of Marine Propeller Performance and Parameters Using CFD Method

Kiam Beng Yeo, Rosalam Sabatly, Wen Yee Hau and Cheah Meng Ong
Materials and Minerals Unit, Faculty of Engineering, Universiti Malaysia Sabah,
Jalan UMS, Kota Kinabalu, 88400, Sabah, Malaysia

Abstract: This study presents the investigation of marine propeller hydrodynamic performance and parameters through Computational Fluid Dynamic analysis. Propellers with different Pitch to Diameter (P/D) ratio, propeller blade number (Z), skew angle, rake angle and Expanded Area Ratio (EAR) were subjected to computational flow analysis based on the Reynolds Averages Navier-Strokes Equation-(RANSE) solver. Results found that all thrust coefficient (K_T) and torque coefficient 10 (K_Q) decreases with the increasing advance coefficient (J). The efficiency of propeller performance had also consistently showed characteristic trend of nonlinear increases to a peak an optimum value before decreasing drastically with increasing J value. The analysis found that no single marine propeller achieve optimum performance in thrust, torque, efficiency and velocity with less loading on the mechanical properties.

Key words: Marine propeller, computational fluid dynamics, flow velocity

INTRODUCTION

A good propeller is required to produce the best hole-shot, high stability and efficiency for a ship movement to be adequate in the range of operations either fast speed and light load, or low speed and heavy load. Nevertheless, manufacturer's propeller series are vast and complex to be fully understood without real involvement of users in the development. Researches are continuously working on the entire reasons and effects of marine propeller to solve for the enhancement of hydrodynamics flow behaviors by refining the propeller shape profile.

Mihaela (2005) and Miyata (1997) found that Computational Fluid Dynamics (CFD) of Solidworks had a numerical algorithm capable of performing hydrodynamic analysis. It decomposed the spatial domain into tiny cells to form the volume mesh and a suitable algorithm was applied to solve the equation of motion (Wu, 2010). In Bertram (2010) research, however, he sectioned the flow analysis of CFD into two parts, which are computer based simulation of fluid flow modeled by field equations and fluid domain. On the other hand, Subhas *et al.* (2012) computed an estimation of thrust and torque performance for different rotational speeds found an extremely ideal CFD result when compared with the experimental work.

Liu *et al.* (2012) had also suggested that uncertainty in CFD analysis had lowered the thrust and torque performance by 5% could be utilized as the standard deviation of measurement of computational value. They further suggested that BEM code has the most reliable method in obtaining potential flow results. They attributed the variance in CFD result as due to software code lacking grid density or too much of numerical dissipation in the vicinity of cavity-fluid interface.

PROPELLER PERFORMANCE ANALYSIS, PARAMETERS AND SETTINGS

Marine propeller hydrodynamic characteristics: Hydrodynamic flow characteristics are important to the complete design of propellers as well as the ship. The hydrodynamic interactions with the propeller provided a series of phenomenon that are related to the physical properties. Dimensionless analysis of propeller performance in terms of thrust coefficient (K_T), torque coefficient (K_Q) and efficiency (η) with respect to advance coefficient, J are standard parameters to evaluate the efficiency of a propulsion system (Mehdi *et al.*, 2010) related as:

$$K_T = \frac{T}{pN^2D^4} \quad (1)$$

$$K_Q = \frac{Q}{pN^2D} \quad (2)$$

$$J = \frac{V_a}{ND} \quad (3)$$

Corresponding Author: Kiam Beng Yeo, Materials and Minerals Unit, Faculty of Engineering, Universiti Malaysia Sabah, Jalan UMS, Kota Kinabalu, 88400, Sabah, Malaysia

where, T is the Thrust, Q is the Torque, P is the Density of fluid, N is the Rotational speed, D is the Diameter and V_a is the Speed of advance. According to Carlton (2007), propeller performance efficiency could be normalized as an optimum curve indicating increasing trend and decreases over a peak value. In most studies, J as the forward movement of propeller with respect to its diameter and rotational speed to determine the efficiency, thrust and torque coefficient was used. The performance was normalized as a characteristic efficiency to identify the optimum parameters for the propeller. Further, he also showed that the values of K_T and K_Q were decreased with with increasing J. The result of John showed similar findings by other researchers on other marine propeller series and experimental models (Mehdi *et al*., 2010).

Computational analysis settings: The CFD analysis and simulation of marine propeller performance under hydrodynamic fluid interaction was conducted. The propeller geometry was generated according to specification before CFD flow simulation set up. An accurate and complete path of setup was required to obtain relevant simulation result. Selection excluding cavities and internal space also reduces time consumption in the CFD computation. Since the actual operating environment of marine propeller was seawater, hence, dynamic similarities were selected at 24°C with a viscosity of 9.11×10^{-4} pa.sec. In the analysis, wall roughness was assumed at 0 μm or smooth, which excluded the pollutant dispersion and deposition; assuming ideal flow characteristic. Thermodynamic parameter of initial standard atmospheric pressure of 101,325 Pa with activation of pressure potential allows incremental computation of depths in the domain of marine propeller. Also, the temperatures of fluid and solid were adjusted according to the actual investigation condition.

Solidworks Flow Simulation does not provide initial setup of solid Computer Aided Design (CAD) model with velocity parameter, except for rotating regions and velocity of flow, which acts perpendicular to the back surface of marine propeller controlled by domain wall initial speed. This was sufficient for propeller-fluid interaction to assimilate the real operation condition. Result and geometry resolution by initial setting allows control of analysis and meshing accuracy, which was time and memory capacity dependent. The governing solution accuracy grossly depends on the geometry resolution governed by computational mesh settings in the minimum gap size, minimum wall thickness and mesh number in the computational domain.

PROPELLER FLOW VELOCITY PERFORMANCE AT DIFFERENT RPM

Flow velocity of different Z at various RPM: Flow velocity against rotational speed with number of blades at Z = 2, 3, 4 and 5 of Fig. 1, Z = 5 reached 18.4 m sec^{-1} and Z = 2 at 15.7 m sec^{-1} in 6000 rpm consisting of 17.2% of variance displacement per unit of time. At initial startup, the higher the Z number, the more rotation was required to achieve the equivalent speed. However, after attaining steady rotation, higher Z emerged as the best blade numbers that bites most water in providing the highest velocity for each rpm. Although higher Z provided better velocity, but it leads to higher fuel consumption and so reduce the efficiency (η).

Flow velocity of different EAR at various RPM: For the velocity and RPM with different EAR (Fig. 2), the smallest value being related to the lowest flow velocity of EAR = 0.3 and 15.7 m sec^{-1} followed by EAR = 0.4 at 16.3 m sec^{-1}, EAR = 0.5 at 17 m sec^{-1}, EAR = 0.6 at 17.6 m sec^{-1} and highest with EAR = 0.7 at 17.9 m sec^{-1}. Increasing the EAR from 30-70% could only increase 14% of flow velocity, while increasing the propeller swipe area by 133%. In terms of geometry, higher the EAR means a heavier weight and more fuel consumption for each rotation.

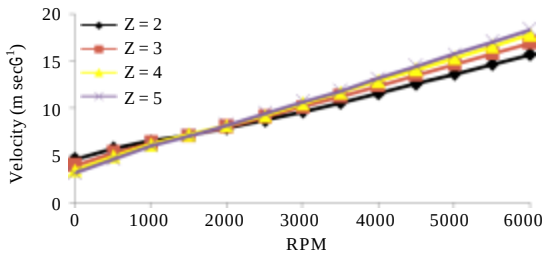

Fig. 1: Flow velocity against RPM for different Z

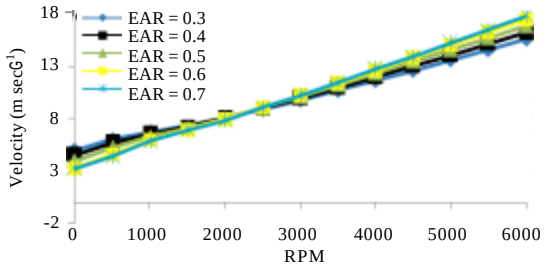

Fig. 2: Flow velocity against RPM for different EAR

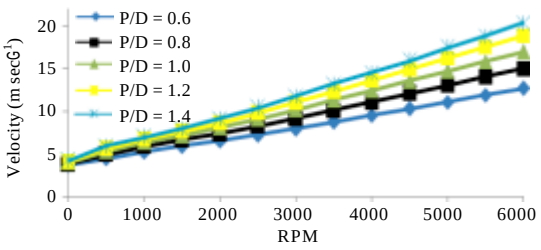

Fig. 3: Flow velocity against RPM for different P/D ratio

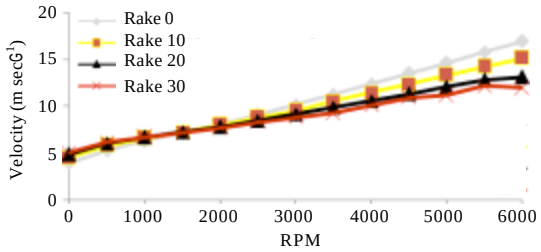

Fig. 4: Fow velocity against RPM with different rake angles

Flow velocity of different P/D ratio of propellers at various RPM: In Fig. 3, linear increasing pitch-diameter ratio occurs with increase rotational speed. Fluid to solid blade surface interaction at zero rpm had a low P/D = 0.6 at 3.6 m sec^{-1} and highest P/D = 1.4 at 4.2 m sec^{-1}. Increasing P/D ratio with higher startup velocity was attributed to the inclined pitch angle to horizontal axis, where blades mounted on the root had reduced the projected area to cause lower thrust of fluid flow acting on the blade. The optimum range of operation speed in most commercial propeller, P/D = 1.4 had achieved the highest speed of 20.33 m sec^{-1} and P/D = 0.6 the lowest at 12.7 m sec^{-1}.

Flow velocity of different rake angle at various RPM: Rake angle measures the degree propeller blade-angle being perpendicular to the hub. Blade rake increases as the blade-face slants backward to the propeller rear ship aft, which was positive rake angle were studied. Results, showed lower rake angle of 0° and 10° linearly increased with higher rpm (Fig. 4). As rake angle increased at higher rotational speed, the numerical values of velocity became unstable. Previous studies suggested that tunnel boats and air entrapment hulls could be unstable for high rake propeller and most propellers had rake angle of 0-20° only.

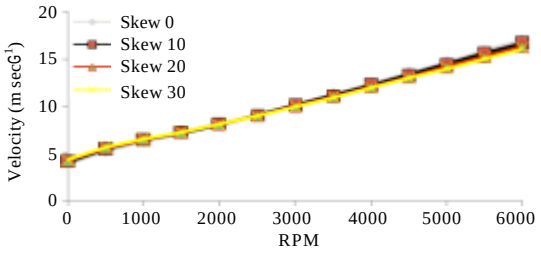

Fig. 5: Flow velocity against RPM for different skew angle

Flow velocity of different skew angle at various RPM: Skew angle measures the degree of the generator line relative to the shaft of a blade section. Velocity of marine propeller with respect to different skew angle of 0-30° had shown an increasing velocity curve with respect to the RPM. Net decreasing velocity with increasing skew angle in propeller design had not provided higher velocity value in this analysis. Instead, the changes of skew had only caused small velocity reduction over the whole operation range (Fig. 5).

PROPELLER PERFORMANCE AND OPERATING PARAMETERS

For convenient comparison between one propeller geometry to another, propeller performance had been defined in non-dimensional parameters. From the particular operating parameters with respect to one another, it was recommended to combine all these parameters in a master graph presented in the following results.

$10K_Q$, K_T and η for various Z with different J: From the CFD analysis, changes of blade numbers for standard propeller geometry of EAR = 0.5, P/D = 1.0, 0° rake angle and 0° skew angle showed that all propeller optimum η values occurred at about 0.78 of J (Fig. 6). For Z = 2, peak performance was achieved at more than 63%, Z = 3 at 61.3%, Z = 4 at 60.8% and Z = 5 at 57.6%. For $10K_Q$ at peak η, Z = 2 was achieved at more than 19.4%, Z = 3 at 24.5%, Z = 4 at 29% and Z = 5 at 30.85%. On the other hand, K_T at peak η for Z = 2 achieved at 9.4%, Z = 3 at 11.9%, Z = 4 at 13.5% and Z = 5 at 13.95%. For the best Q to η and T to η values, it was only relevant at the point when decreasing curve $10K_Q$ and K_T first hit the η curve. The Q, T and η best intersection point for each Z-parameter were shown in Table 1. All Z had η curves showed rapid increase from 0 rpm and decreased steadily after the peak η, while 10 K_Q and K_T decreases as J starts to increase.

$10K_Q$, K_T and η for various EAR with different J: Marine propeller profile for Z = 3, P/D = 1.0, 0° of skew angle and 0° of rake angle with changes of EAR from 0.3-0.7 were conducted, Fig. 7. The performance curve of best η for EAR = 0.4 had the highest 62.4% followed by EAR = 0.5 at 61.25%, EAR = 0.3 at 59.22%, EAR = 0.7 at 58.37% and EAR = 0.6 at lowest value of 56%. Best performance for intersection of $10K_Q$, K_T, η was also displayed in Table 2. All trend of η curves were increasing to peak at J = 0.8 before decreasing drastically. Also, Q and T performances were decreased with the increment of J with higher EAR decreased much faster than lower one. $10K_Q$ and K_T values were initially higher at larger EAR ratio, but smaller EAR profiles took over larger ones after crossing the peak efficiency curve at J = 0.8.

Table 1: Best performance of Q-T-η parameters for different Z

Z	Q-η	T-η
2	38.2% at J = 0.379	27.2% at J = 0.259
3	43.6% at J = 0.452	30.9% at J = 0.313
4	46.9% at J = 0.498	33.4% at J = 0.339
5	48.5% at J = 0.529	34.6% at J = 0.359

Table 2: Best performance of Q-T-η parameters for different EAR

EAR	Q-η	T-η
0.3	39.6% at J = 0.398	27.8% at J = 0.272
0.4	42.1% at J = 0.427	29.5% at J = 0.293
0.5	43.6% at J = 0.452	30.8% at J = 0.313
0.6	44.7% at J = 0.486	31.8% at J = 0.331
0.7	47.1% at J = 0.473	34.3% at J = 0.342

$10K_Q$, K_T and η for various P/D ratio with different J: From the Fig. 8, each P/D ratio profile had a peak η with respect to the J. Instead, $10K_Q$, K_T value for all P/D profiles were varied with different values over the η curve and decreased smoothly with respect to J. As the P/D ratio went higher, the efficiency value also increased; highest efficiency for various P/D ratio in this result was 1.4 achieved at more than 67%, followed by P/D = 1.2 at 61.5%, P/D = 1.0 at 61%, P/D = 0.8 at 59% and the lowest was P/D = 0.6 at 54%. The trend of $10K_Q$ and K_T to η, low P/D ratio propeller intersected the η curves at lower figures and higher P/D ratio to achieve at greater one. The optimum performance of Q and T when it first intersected the η curve was displayed in Table 3.

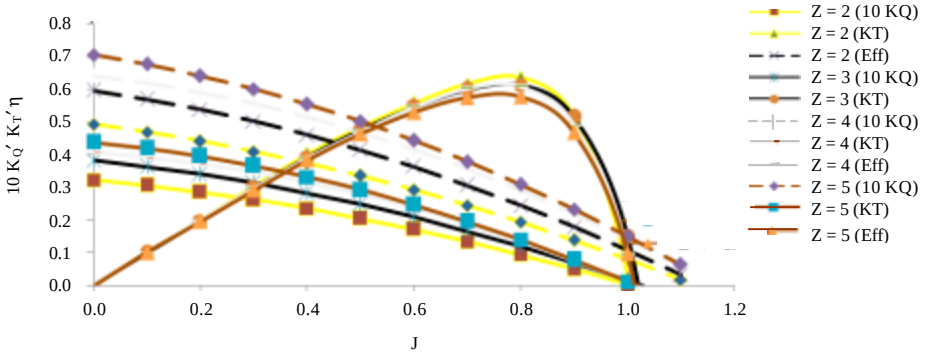

Fig. 6: Graph of 10 K_Q, K_T, η with respect to J for different Z

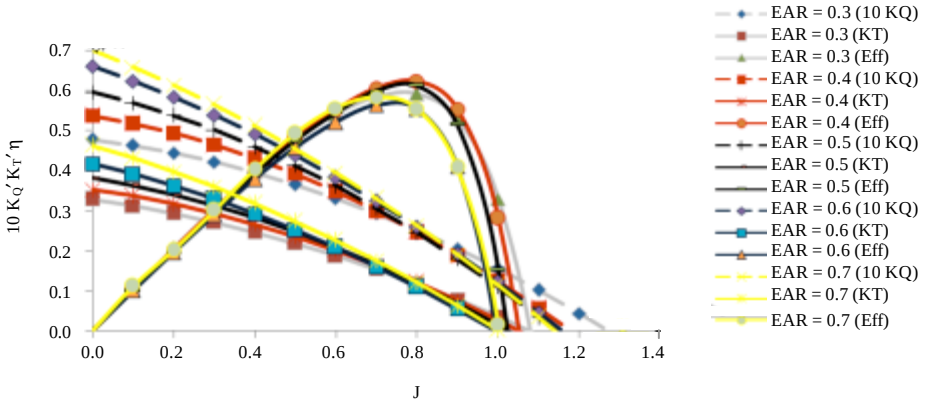

Fig. 7: Graph of 10 K_Q, K_T, η with respect to J for different EAR values

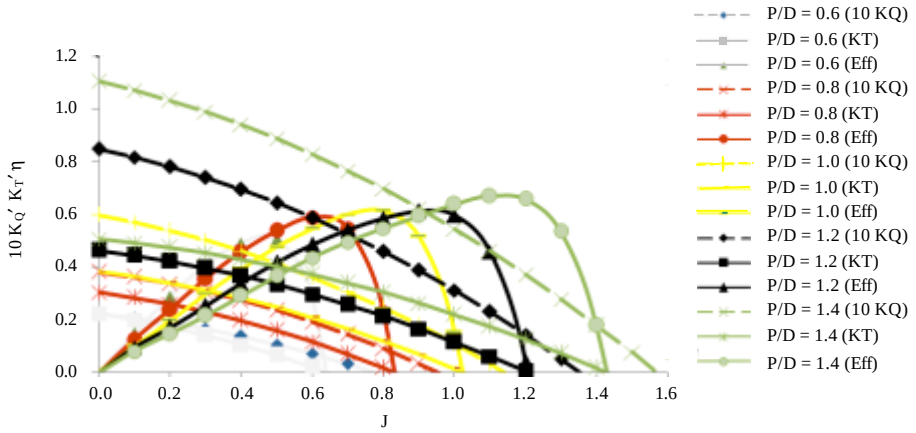

Fig. 8: Graph of 10 K_Q, K_T, η with respect to J for different P/D ratio

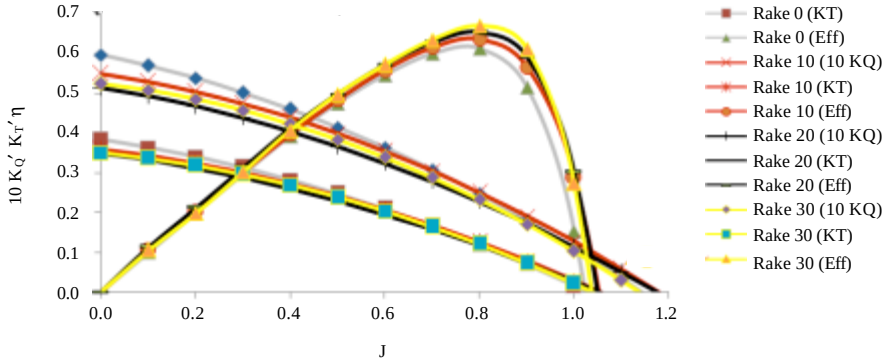

Fig. 9: Graph of 10 K_Q, K_T, η with respect to J for different rake angle

Table 3: Best performance of Q-T-η parameters for different P/D ratio

P/D	Q-η	T-η
0.6	20.72% at J = 0.127	19.11% at J = 0.131
0.8	31.81% at J = 0.266	25.57% at J = 0.213
1.0	43.63% at J = 0.452	30.91% at J = 0.312
1.2	53.34% at J = 0.688	35.82% at J = 0.425
1.4	60.38% at J = 0.924	39.17% at J = 0.537

Table 4: Best performance of Q-T-η parameters for different rake angle

Rake (°)	Q-η	T-η
0	43.63% at J = 0.452	30.88% at J = 0.313
10	42.57% at J = 0.432	29.99% at J = 0.298
20	40.5% at J = 0.3950	29.14% at J = 0.290
30	41.81% at J = 0.412	29.61% at J = 0.296

Table 5: Best performance of Q-T-η parameters for different skew angle

Skew Angle (°)	Q-η	T-η
0	43.63% at J = 0.452	30.9% at J = 0.313
10	44.11% at J = 0.457	31.4% at J = 0.316
20	44.65% at J = 0.465	31.5% at J = 0.318
30	45.55% at J = 0.467	32.0% at J = 0.324

10K_Q, K_T and η for various rake angle with different J: The Fig. 9 analyses the propeller performance for 0-30° rake angle of propeller profile with Z = 3, EAR = 0.5, 0° skew angle and P/D=1.0. The η curve were increasing to reach optimum performance at J = 0.8, before drastically decreased to J value at 1.1. Higher skew angle had achieved the best η but not for the intersection point for 10 K_Q, K_T and η, Table 4. The 0° rake angle had the highest value of Q to η followed by 10°, 30° and finally 20° with the lowest net Q value. The phenomena of Q to η also similarly occurred to the K_T characteristics curve. Table 4 displayed the best Q and T results at the first intersection with the η curve.

10K_Q, K_T and η for various of skew angle with different J: The Fig. 10 with various skew angles for Z = 3, EAR = 0.5, P/D = 1.0 and 0° of rake angle had increasing efficiency before drastic decreased right after the J = 0.8, while the 10 K_Q and K_T decreased with increasing J values. At 30° of skew angle, the highest η value was achieved at 65%, followed by skew 20° with 62.97%, skew 10° with 62.55% and the lowest was zero skew angle with 61.25%. Best performance for intersection of 10 K_Q, K_T and η was displayed in Table 5.

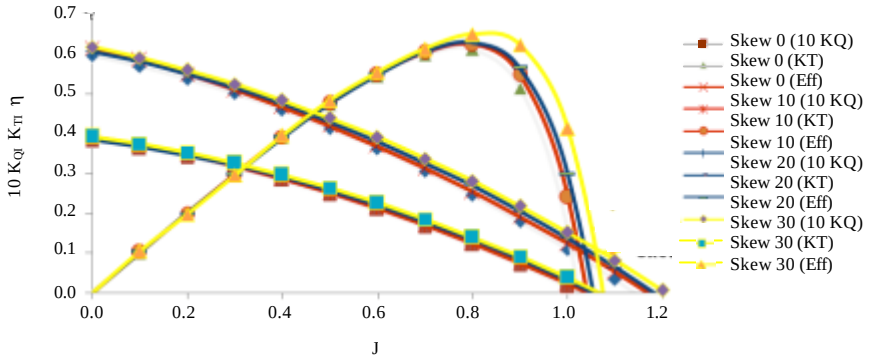

Fig. 10: Graph of 10 K_Q, K_T, η with respect to J for different skew angle

CONCLUSION

The performances and parameters investigation were conducted by implementing the computational fluid dynamics and finite element analysis to a standard set of marine propeller geometry. Results had shown that all K_T and 10 K_Q dropped with the increasing of J values. Furthermore, the efficiency of the propeller had increased at a small inclination before an optimum peak value was achieved and then to drop drastically right after with increasing Advance Coefficient J. Finally, no single marine propeller could achieve a single optimum performance in thrust, torque, efficiency and velocity with less loading on its mechanical properties.

ACKNOWLEDGEMENT

The authors would like to express their appreciation to the Materials and Mineral Unit, Faculty of Engineering, Universiti Malaysia Sabah and the Ministry of Higher Education of Malaysia for the financial support through the research grant FRG0249-TK-2/2010 and FRG0247-TK-2/2010.

REFERENCES

Bertram, V., 2010. Appropriate tools for flow analyses for fast ships. Germanischer Lloyd, Hamburg, Germany.

Carlton, J.S., 2007. Marine Propellers and Propulsion. 2nd Edn., Butterworth-Heinemann, Oxford, UK.

Liu, D., F. Hong, F. Zhao and Z. Zhang, 2012. The CFD analysis of propeller sheet cavitation. China Ship Scientific Research Center, Wuxi, China.

Mehdi, N., M.J. Abbasi and A.M. Amini, 2010. Assessment of marine propeller hydrodynamic performance in open water via CFD. Proceedings of the International Conference on Marine Technology, December 11-12, 2010, Dhaka, Bangladesh, pp: 35-44.

Mihaela, A., 2005. Developments in the design of ship propeller. Scientific Bulletin of the Politehnica University of Timisoara Transactions on Mechanics, University of Galati.

Miyata, H., 1997. Time-marching CFD simulation for moving boundary problems. Proceedings of the 21st Symposium on Naval Hydrodynamics, June 24-28, 1996, Trondheim, Norway.

Subhas, S., V.F. Saji, S. Ramakrishna and H.N. Das, 2012. CFD analysis of propeller flow and cavitation. Int. J. Comput. Applic., 55: 26-33.

Wu, X., 2010. A Rapid Development Process for Marine Propellers through Design, Simulation and Prototyping. Memorial University of Newfoundland, St. John's, Newfoundland and Labrador, Pages: 244.